Thermal Properties and Isothermal Crystallization of Syndiotactic Polypropylenes: Differential Scanning Calorimetry and Overall Crystallization Kinetics

PITT SUPAPHOL,* JOSEPH E. SPRUIELL

Center for Materials Processing and Department of Materials Science & Engineering, University of Tennessee, 434 Dougherty Engineering Building, Knoxville, Tennessee 37996-2200

Received 16 February 1999; accepted 16 April 1999

ABSTRACT: Isothermal crystallization and subsequent melting behavior of five samples of syndiotactic polypropylene are presented. Crystallization studies were carried out in the temperature range of 60°C to 97.5°C using a differential scanning calorimeter (DSC). Subsequent DSC scans of isothermally crystallized samples exhibited double melting endotherms. The high melting peak was concluded to be the result of the melting of crystals formed by recrystallization during the reheating process. Overall crystallization kinetics was studied based on the traditional Avrami analysis. Analysis of crystallization times based on the modified growth rate theory suggested that, within the crystallization temperature range studied, the syndiotactic polypropylenes crystallize in regime III. Kinetic crystallizability parameters also were evaluated, and were found to be in the range of 0.41°C s^{-1} to 2.14°C s^{-1}. © 2000 John Wiley & Sons, Inc. J Appl Polym Sci 75: 44–59, 2000

Key words: syndiotactic polypropylene; isothermal crystallization; multiple melting endotherms; regime crystallization

INTRODUCTION

Since the mid-1950s, the invention of Ziegler–Natta catalysis[1–3] has opened up a new era in the synthesis of polyolefins. In 1958, isotactic polypropylene (i-PP) was successfully synthesized, and later became one of the most widely used and studied polymers. In the 1960s, the syndiotactic form of polypropylene was successfully synthesized[4,5] based on the AlR_2Cl/VCl_4 catalyst systems. Even though the resulting polymer possessed a fair level of syndiotactic content, it contained too high a level of regio-irregular defects (e.g., head-to-head/tail-to-tail type defects). As a result, the properties of the obtained polymer were inferior to those of its isotactic counterpart.

In 1988, Ewen et al.[6] reported that highly stereoregular and regioregular s-PP can be polymerized using a catalyst system composed of isopropylidene(cyclo-pentadienyl)(9-fluorenyl)zirconium or hafnium dichloride and methylaluminoxane. The discovery of these new metallocene catalyst systems helped open up a new route for the production of s-PP with much improved purity and yields and produced renewed interest in the properties and possible applications of this "second generation" s-PP.

It is well known that molecular characteristics, such as molecular weight, molecular weight distribution, stereoregularity, and regioregularity greatly influence the crystallization behavior and resulting morphology of polymers. It is therefore

* *Present address:* The Petroleum and Petrochemical College, Chulalongkorn University, Soi Chulalongkorn 12, Phyathai Road, Pathumwan, Bangkok 10330, Thailand.

Correspondence to: J. E. Spruiell.

Journal of Applied Polymer Science, Vol. 75, 44–59 (2000)
 CCC 0021-8995/00/010044-16

necessary to understand and obtain enough information on basic crystallization characteristics of the polymers of interest before further studies are carried out. In this paper, we examine the isothermal bulk crystallization kinetics as well as melting behavior of s-PPs, using a differential scanning calorimeter.

THEORETICAL BACKGROUND

Bulk isothermal crystallization kinetics was studied by following the exotherms recorded in the DSC7. When used to follow the crystallization of polymers, what DSC measures is the heat flow released due to the exothermic nature of the crystallization process. The heat flow $\dot{Q}$ is directly proportional to the weight of the sample w, the enthalpy of crystallization ΔH_c, and the overall crystallization rate $\dot{\theta}(t)$. Theoretically, ΔH_c is a product of the absolute crystallinity χ_c and the crystallization enthalpy of an infinitely thick extended chain crystal of a perfect crystal (i.e. 100% crystallinity) ΔH_c°. Ideally, ΔH_c° is also equal to the enthalpy of fusion of a perfect crystal ΔH_f°; thus, they can be used interchangeably. Consequently, we may write the equation of heat flow as

$$\dot{Q} \propto w \cdot \chi_c \cdot \Delta H_f^\circ \cdot \dot{\theta}(t). \tag{1}$$

By setting $\dot{q} = \dot{Q}/(c_1 \cdot w \cdot \chi_c \cdot \Delta H_f^\circ)$ (where c_1 is a proportionality constant), the relative crystallinity as a function of time $\theta(t)$, can be obtained by integrating the normalized heat flow (t), over the course of the crystallization process. One finally gets

$$\theta(t) = \int_0^t \dot{\theta}(t)\, dt = \int_0^t \dot{q}(t)\, dt. \tag{2}$$

Analysis of isothermal bulk crystallization kinetics is usually performed using the Avrami equation,[7] which is normally written in the form:

$$\theta(t) = 1 - \exp(-kt^n), \tag{3}$$

where k denotes the bulk crystallization rate constant, and n the Avrami exponent. Both k and n are constants typical of a given morphology and primary nucleation type. It should be noted that t is the time spent during the course of crystallization measured from the onset of crystallization (the incubation time is excluded). In practice, eq. (3) is usually written in its logarithmic form:

$$\ln[-\ln(1 - \theta(t))] = \ln k + n \ln(t). \tag{4}$$

According to eq. (4), when plotting $\ln[-\ln(1-\theta(t))]$ against $\ln(t)$, the values of n and k can readily be extracted and taken as the slope and the antilogarithmic value of the y-intercept, respectively.

Based on eq. (3), if the time the polymer spends from the beginning of the crystallization process to the time at which a certain amount of relative crystallinity has developed is known (denoted t_θ: e.g., if $\theta = 0.50$, $t_{0.5}$ is the half-time of crystallization), k can also be directly calculated. By rearranging eq. (3), one arrives at

$$k = \frac{-\ln(1 - \theta)}{t_\theta^n}. \tag{5}$$

If $\theta = 0.5$, eq. (5) converts into a more familiar equation, which reads

$$k = \frac{\ln 2}{t_{0.5}^n}. \tag{6}$$

Since the crystallization time t_θ can be obtained directly from the experimental data, it can be adapted to investigate the regime behavior (based on the growth rate theory by Hoffman et al.[8,9]) in the isothermal crystallization of polymers, as described below. According to the Lauritzen and Hoffman theory, the spherulite growth rate G is given as

$$G = G_0 \exp\left(-\frac{U^*}{R(T_c - T_\infty)} - \frac{K_g}{T_c(\Delta T)f}\right), \tag{7}$$

where G_0 is a preexponential term that is not strongly dependent on temperature. U^* is the activation energy of the elementary jump process, which governs the mobility of the polymer with respect to the temperature and is commonly given by a universal value of 6,276 J mol^{-1},[8] T_c is the crystallization temperature, T_∞ is the temperature where the molecular reptation is essentially zero and is frequently assumed to be $T_g - 30$, R is the gas constant, ΔT is the degree of undercooling ($T_m^\circ - T_c$), and f is a factor used to correct for the temperature dependence of the heat of fusion, which is denoted $2T_c/(T_c + T_m^\circ)$. It should be noted that U^* and T_∞ are the WLF (Williams–Landel-

Table I Characterization Data of As-Received Syndiotactic Polypropylene Samples

Sample	Intrinsic Viscosity (dL g^{-1})	M_n	M_w	M_z	M_w/M_n	Racemic Pentads [%rrrr]	Racemic Triads [%rr]	Racemic Dyads [%r]	Ethylene Content (% by wt)
s-PP#1	1.61	76 200	165 000	290 000	2.15	77.10	87.31	91.42	1.3
s-PP#2	1.80	52 300	195 000	450 000	3.73	74.55	83.09	87.36	0.6
s-PP#3	1.32	37 300	133 000	308 000	3.55	74.61	83.73	88.29	0.5
s-PP#4	1.61	81 300	171 000	294 000	2.10	74.63	84.37	89.24	0.3
s-PP#5	1.52	47 000	165 000	406 000	3.51	75.28	85.09	90.00	0.2

Ferry) parameters. K_g is the nucleation exponent, and is defined as

$$K_g = \frac{jb_0\sigma\sigma_e T_m^\circ}{k\Delta H_f^\circ}, \quad (8)$$

where j equals 2 for regime II and 4 for regimes I and III, b_0 denotes the crystal layer thickness along the growth direction, σ and σ_e the lateral and fold surface free energy, respectively, T_m° the equilibrium melting temperature, k the Boltzmann's constant, and ΔH_f° the heat of fusion.

In the case of overall crystallization kinetics, the growth rate theory can be applied by use of the following relationship (provided that the nucleation is mainly instantaneous and the growth is spherulitic in nature):

$$k = \frac{4}{3}\pi G^3 N, \quad (9)$$

where N is the number of nucleation sites which is essentially constant for instantaneous nucleation type. Substitution of eq. (7) into eq. (9) and equating the product with eq. (5) gives the following relationship between t_θ and G:

$$t_\theta^{-1} = A_1 G_0 \exp\left(-\frac{U^*}{R(T_c - T_\infty)} - \frac{K_g}{T_c(\Delta T)f}\right), \quad (10)$$

where A_1 is an arbitrary proportionality constant, and

$$\log(t_\theta^{-1}) = A_2 - \frac{U^*}{2.303R(T_c - T_\infty)} - \frac{K_g}{2.303T_c(\Delta T)f}, \quad (11)$$

where $A_2 = \log A_1 + \log G_0$, and

$$\log(t_\theta^{-1}) + \frac{U^*}{2.303R(T_c - T_\infty)} = A_2 - \frac{K_g}{2.303T_c(\Delta T)f}. \quad (12)$$

According to eq. (12), construction of $\log(t_\theta^{-1}) + U^*/2.303R(T_c - T_\infty)$ versus $1/2.303T_c(\Delta T)f$ plot serves as the regime test for the case of instantaneous nucleation with three-dimensional growth. The slope of such a plot is equal to $-K_g$.

EXPERIMENTAL

Materials

The s-PPs used in this study were supplied in the pellet form by Fina Oil and Chemical Company in La Porte, Texas. Molecular characterization of these materials was kindly performed by Dr. Roger A. Phillips and his coworkers at Montell USA, Inc. in Elkton, Maryland. The results are listed in Table I. It should be noted that s-PP#2, s-PP#3, and s-PP#5 exhibit a bimodal molecular weight distribution, which results in an unusually high degree of polydispersity.

Technique and Sample Preparation

A Perkin–Elmer Series 7 Differential Scanning Calorimeter (DSC7) was used to follow the isothermal crystallization as well as related thermal characteristics in this study. The DSC7 equipped with internal liquid nitrogen cooling unit dependably provided a cooling rate up to 200°C min^{-1}. Temperature calibration was performed using indium as a standard; it has the following thermal properties: T_m° = 156.6°C and ΔH_f° = 28.5 J g^{-1}. The consistency of the temperature calibration was checked every other run to ensure reliability

of the data obtained. To make certain that thermal lag between the polymeric sample and the DSC sensors is kept to a minimum, each sample holder was loaded with a single disc, weighing around 4.9 ± 0.3 mg. A hole-puncher was used to cut the disc from a film. The film was prepared by melt-pressing virgin pellets, placed between a pair of Kapton films, which in turn were sandwiched between a pair of stainless steel platens, in a Wabash compression molding machine at 190°C under a pressure of 67 kpsi. After 10 min holding time, the film, approximately 280 μm thick, was taken out and immediately submerged in an ice-water bath, while it was still between the two steel platens. This treatment assumes that previous thermal and mechanical histories were essentially erased and provides a controlled condition for the film.

Methods

The experiment started with heating the sample from −40°C at a scanning rate of 80°C min^{-1} to 190°C min^{-1}, and was held there for 5 min before quenching at a cooling rate of 200°C min^{-1} to a desired isothermal crystallization temperature T_c. The 5-min holding time at 190°C is necessary to erase the previous crystalline and orientation memories. At each crystallization temperature, the crystallization process was closely monitored. It was assumed that the crystallization finished when the exothermic trace converged to a horizontal baseline, at which point the DSC was programmed to quench the sample to T_c − 10°C. After 1-min holding time, the sample was heated at a scanning rate of 20°C min^{-1} to observe its melting behavior. The relationship of the melting point observed and the crystallization temperature was also considered by preparing a Hoffman and Weeks plot.[10] It should also be noted that each experimental run was performed on a fresh sample.

In this study, the glass transition temperature of each s-PP sample was also investigated. The experiment started by melting a sample, which was encapsulated in a DSC sample holder, in a Mettler FP 82 hot stage, the temperature of which was preset at 190°C. After a 5-min holding time, the sample was immediately quenched and submerged in liquid nitrogen for 3 min. The sample was then transferred as quickly as possible to the DSC cell, the temperature of which was preset at −40°C. As soon as the heat flow became stable, the sample was heated at a heating rate of 20°C min^{-1}. The glass transition temperature was then taken as the mid-point of the specific heat jump in the glass transition region.[11]

Table II Glass Transition Temperatures for Syndiotactic Polypropylene Samples

Sample	T_{go} (°C)	T_{ga} (°C)	ΔC_p (J g^{-1} K^{-1})	T_g (°C)
s-PP#1	−8.94	−3.42	0.43	−6.05
s-PP#2	−8.34	−3.81	0.41	−5.98
s-PP#3	−8.84	−4.42	0.42	−6.52
s-PP#4	−8.27	−3.03	0.47	−5.60
s-PP#5	−9.61	−3.73	0.49	−6.47

RESULTS AND DISCUSSION

Glass Transition Temperature

The measured glass transition temperatures are listed in Table II for each sample. Other relevant data are also tabulated, such as the extrapolated glass transition onset T_{go} the extrapolated endpoint T_{ga} and the specific heat jump ΔC_p. According to Table II, ΔC_p lies in the range of 0.41 to 0.49 J g^{-1} K^{-1}. The value of T_g for each sample does not vary much, and it is likely that all values are within experimental error of the average value of −6.1 ± 0.4°C (267.0 ± 0.4 K). The glass transition temperatures of s-PP have been reported by a number of authors. Miller and Seeley[12] used two different methods, DSC and an automated torsional braid, and came up with the values of 0°C and 3°C, respectively. Haftka and Könnecke[13] determined the T_g of an s-PP sample with 92.4% syndiotacticity (racemic pentads) to be 0°C by slow-cooling at 20°C min^{-1} in a DSC. Recently, Eckstein et al.[14] has reported the T_g values of s-PP samples with 79.6% and 92.0% syndiotacticity (racemic pentads) to be 0°C and 3.3°C, respectively, using a DSC. They did the experiment by first quenching the samples at 200°C min^{-1} to −60°C and then determined the T_g values upon subsequent heating at 20°C min^{-1}.

Melting Behavior and Equilibrium Melting Temperature

Figure 1 presents a set of DSC heating thermograms which were collected at a heating rate of 20°C min^{-1} for s-PP≠4 samples isothermally crystallized at specified temperatures. It is appar-

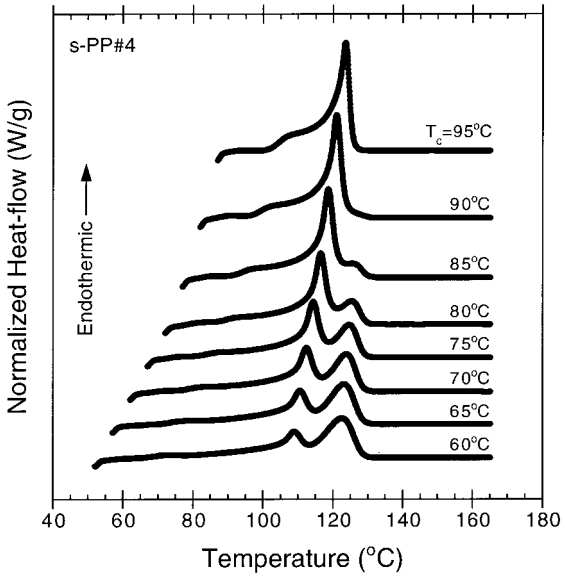

Figure 1 Melting endotherms of sample s-PP#4, recorded at the heating rate of 20°C min^{-1}, after isothermal crystallization at the specified temperature.

ent that the DSC endotherms exhibit double melting peaks, which are distinguishable at crystallization temperature below 90°C. Moreover, with an increase in crystallization temperature, the low melting peak seems to increase in its size and sharpness and moves to a higher temperature. On the contrary, the high melting peak gets smaller as the crystallization temperature increases and disappears when $T_c \geq 90$°C. This is, in general, consistent with earlier published results by other authors.[15–18] Another interesting melting characteristic of s-PP, which can be observed directly from its melting endotherms, is that, upon reheating, the melting starts at a temperature close to its crystallization temperature (ca. $\approx T_c + 7$°C). This phenomenon was verified very recently by Schmidtke et al.[18] It is now believed that the melting starts slightly after T_c[18], and it is followed by a recrystallization[15,18] in the range of the first melting endotherm, resulting in the appearance of the second endotherm. However, the phenomenon is less pronounced at high T_c.

To account for the effect of heating rate on the melting behavior of s-PP, we have performed a separate qualitative experiment on s-PP#4, the result of which is presented in Figure 2. In this experiment, each sample was isothermally crystallized at 75°C, then its melting thermogram was recorded at six different scanning rates, ranging from 5°C min^{-1} to 40°C min^{-1}. It is evident, according to Figure 2, that the areal fraction of the high-melting endotherm decreases with increasing heating rate, while the area of the lower melting peak increases. This finding is in a very good agreement with earlier reports[16–18] and confirms the suggestion that the high-melting endotherm is in fact a result of a recrystallization process that occurred during the melting of the polymer. As was pointed out by Rodriguez–Arnold and coworkers,[16] the heating rate used to obtain a melting endotherm plays a major role in the melting point observed. The observed melting points when the heating rate is either lower or greater than 20°C min^{-1} are greater in value than that obtained at 20°C min^{-1}. They suggested that it is the annealing effect that contributes to the increase in the melting point at the lower heating rates, whereas it is the instrumental thermal lag at the higher heating rates. We also found this similar trend in our result. This is the justification for the experiment to be conducted at the heating rate of 20°C min^{-1}.

Complete experimental data taken from crystallization exotherms and subsequent melting endotherms for all s-PP samples are listed in Table III. It is clearly seen, according to Table III, that peak temperature values T_{mh} of the high-melting endotherms for all s-PP samples are less dependent on the crystallization temperature than those T_{ml} of the low-melting ones. Furthermore, it

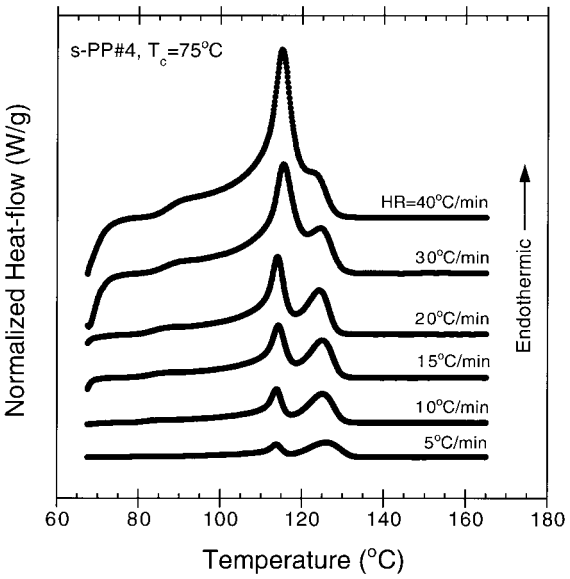

Figure 2 Melting endotherms of sample s-PP#4, recorded at the specified heating rates, after isothermal crystallization at 75°C.

Table III Crystallization and Melting Data for Syndiotactic Polypropylene Samples

Sample	s-PP#1				s-PP#2				s-PP#3				s-PP#4				s-PP#5			
T_c (°C)	ΔH_c (J g^{-1})	ΔH_f (J g^{-1})	T_{ml} (°C)	T_{mh} (°C)	ΔH_c (J g^{-1})	ΔH_f (J g^{-1})	T_{ml} (°C)	T_{mh} (°C)	ΔH_c (J g^{-1})	ΔH_f (J g^{-1})	T_{ml} (°C)	T_{mh} (°C)	ΔH_c (J g^{-1})	ΔH_f (J g^{-1})	T_{ml} (°C)	T_{mh} (°C)	ΔH_c (J g^{-1})	ΔH_f (J g^{-1})	T_{ml} (°C)	T_{mh} (°C)
60.0	27.9	33.6	110.3	124.1	—	—	—	—	—	—	—	—	—	—	—	—	—	—	—	—
62.5	28.0	34.4	111.0	124.4	—	—	—	—	—	—	—	—	—	—	—	—	—	—	—	—
65.0	28.0	35.7	112.0	124.9	—	—	—	—	—	—	—	—	—	—	—	—	—	—	—	—
67.5	28.7	35.7	112.8	125.2	—	—	—	—	—	—	—	—	—	—	—	—	—	—	—	—
70.0	29.3	35.9	113.7	125.5	—	—	—	—	—	—	—	—	26.5	33.0	112.4	123.8	30.3	36.6	113.9	127.0
72.5	30.1	35.9	114.6	125.8	28.2	35.2	113.4	124.5	28.4	36.0	113.2	125.8	27.1	33.2	113.3	124.3	31.5	37.4	114.7	127.3
75.0	30.7	36.0	115.5	126.2	29.2	35.2	114.5	125.2	29.4	36.1	114.2	126.2	28.4	33.3	114.3	124.6	31.9	37.8	115.5	127.6
76.5	—	—	—	—	—	—	—	—	—	—	—	—	—	—	—	—	32.1	37.8	116.1	127.8
77.5	31.5	36.3	116.2	126.1	29.7	35.2	115.4	125.5	29.9	36.2	115.6	127.0	28.7	33.3	115.5	125.3	32.5	38.4	116.8	128.4
80.0	31.9	36.3	117.2	126.4	30.9	35.5	116.3	125.5	30.3	36.2	116.2	127.1	29.0	33.4	116.4	125.3	32.6	38.6	117.7	128.7
82.5	32.1	36.5	118.2	126.9	32.0	35.5	117.3	126.1	32.3	36.5	117.4	127.5	29.6	33.4	117.6	125.6	33.5	38.8	118.6	129.1
85.0	33.4	37.4	119.4	127.1	32.7	35.7	118.6	126.4	32.4	36.6	118.5	127.9	29.8	33.4	118.6	125.6	33.5	38.9	119.6	129.5
86.0	—	—	—	—	—	—	—	—	—	—	—	—	30.1	33.5	119.3	—	33.6	39.4	120.2	129.7
87.5	34.5	37.6	121.0	—	33.6	35.8	119.8	—	33.0	36.8	120.3	128.7	30.5	33.6	120.1	—	34.1	39.6	120.9	129.9
88.0	—	—	—	—	—	—	—	—	—	—	—	—	30.7	33.8	120.1	—	—	—	—	—
90.0	35.2	38.0	122.2	—	34.9	35.9	120.9	—	33.8	37.1	120.9	128.7	32.7	34.0	121.0	—	34.6	40.1	122.0	130.2
91.5	—	—	—	—	—	—	—	—	—	—	—	—	—	—	—	—	34.7	40.3	122.8	130.6
92.5	35.5	39.2	123.6	—	35.5	36.2	122.1	—	34.5	37.2	122.3	129.0	32.8	34.3	122.4	—	34.8	40.7	123.0	130.4
95.0	36.1	39.8	125.0	—	36.2	37.5	123.8	—	35.2	37.8	123.7	—	34.2	34.5	123.6	—	35.1	40.9	124.4	—
97.5	—	—	—	—	—	—	—	—	—	—	—	—	—	—	—	—	35.4	41.1	125.7	—

is apparent that both enthalpy of crystallization ΔH_c and enthalpy of fusion ΔH_f increases with increasing T_c, whereas the difference between the two quantities decreases. For example, for s-PP#1 the difference between ΔH_f and ΔH_c is as much as 20.4% at T_c = 60°C, as opposed to 10.2% at T_c = 95°C; and for s-PP#5 it is 20.5% at T_c = 70°C, as opposed to 16.2% at T_c = 97.5°C. Along with the result shown in Figure 2, this suggests that the low-melting endotherms most likely are a result of the crystals formed at T_c, whereas the high-melting ones are a result of the recrystallization of metastable crystals melted in the course of the first melting peak. It also suggests that the once-molten crystals are less likely to recrystallize when T_c is increased. In addition to the hypothesis of recrystallization effect, the temperature dependence of ΔH_f may, to some extent, account for the difference between ΔH_f and ΔH_c.[18]

Based on the hypothesis drawn previously that the values of the low-melting peaks correspond to the melting of the crystals formed at a specified T_c, the T_{ml} values listed in Table III are now considered as the melting points T_m of the samples crystallized at T_c. According to a theory derived by Hoffman and Weeks,[10] the equilibrium melting temperature T_m°, that is the melting temperature of infinitely extended crystals, can be obtained by linear extrapolation of T_m versus T_c data to the line $T_m = T_c$. Mathematically, they arrived at the following equation:

$$T_m = \frac{T_c}{2\beta} + T_m^\circ\left[1 - \frac{1}{2\beta}\right], \qquad (13)$$

where β is the "thickening ratio." In other words, β indicates the ratio of the thickness of the mature crystal L_c to that of the initial one L_c^*; therefore, $\beta = L_c/L_c^*$, which is supposed to always be greater than or equal to 1. It should be noted that the factor 2 in eq. (13) suggests that the thickness of the crystals undergoing melting is approximately doubled that of the initial critical thickness.

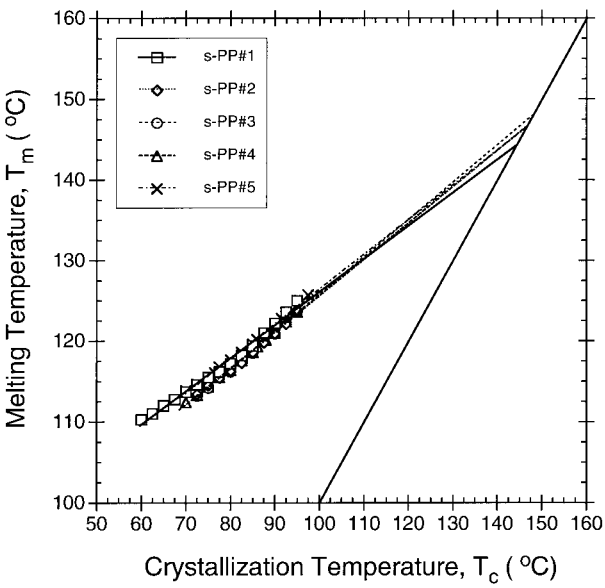

Figure 3 Melting temperatures as a function of crystallization temperatures for the s-PP samples.

Figure 3 shows the plots of T_m versus T_c for all s-PP samples. It is evident that T_m values for all of the samples exhibit a linear relationship with T_c, at least in the temperature range of interest. The intersection of a least square line, fit to the data set for each sample, with the line $T_m = T_c$ provides the values of T_m°. The slope of the least square line, which equals $1/2\beta$, can also be used to calculate the β parameter (i.e., $\beta = 0.5 \times \text{slope}^{-1}$). These values, along with the correlation coefficient, r^2, of the fit, are reported in Table IV. The results show that the T_m° values lie between 146.1°C and 148.3°C (419.3 K and 421.4 K). The slopes of the least square lines range from 0.41 to 0.47, which agree extremely well with the published result by Balbontin et al.[19] Derived from

Table IV Thermodynamic Equilibrium Melting Points, β Parameters, and Corresponding Calculated Equilibrium Melting Points for 100% Syndiotacticity for Syndiotactic Polypropylene Samples

Sample	[%rrrr]	[%rr]	[%r]	T_m° (°C)	T_m° (K)	Slope	β	r^2	$(T_m^\circ)_{100\%}$ (°C)	$(T_m^\circ)_{100\%}$ (K)
s-PP#1	77.10	87.31	91.42	146.1	419.3	0.41	1.2	0.988	163.2	436.3
s-PP#2	74.55	83.09	37.36	146.6	419.7	0.45	1.1	0.994	172.9	446.0
s-PP#3	74.61	83.73	88.29	148.3	421.4	0.47	1.1	0.995	172.6	445.7
s-PP#4	74.63	84.37	89.24	146.4	419.5	0.45	1.1	0.998	168.3	441.4
s-PP#5	75.28	85.09	90.00	146.4	419.5	0.43	1.2	0.997	166.6	439.7

the slopes of the least square lines, the lamellar thickening parameter β is found to be roughly 1, which is in a very good agreement with other reports.[13,19] In addition, the value of β near 1 guarantees that the extrapolation is valid and gives a reliable T_m° value, since the T_m values observed for different T_c values are not affected greatly by the annealing process.

There are a number of reported values of T_m° available in the literature.[12,13,15–21] These values scatter in a wide range, depending on the syndiotacticity level of the sample used. By lacking a common basis of reporting the degree of syndiotacticity, it is quite difficult to compare the reported values together. Recently, the level of NMR racemic pentads [*%rrrr*] has been used more frequently to represent the degree of syndiotacticity in s-PP samples. Therefore, only those published T_m° values with known [*%rrrr*] will be reported with the syndiotacticity level in parentheses: they are 168°C (92%),[15] 160°C (86%),[16] 155°C to170°C (87% to 95%),[17] 166°C (91%),[18] and 150°C to 186°C (89% to 95%).[19] Comparing with these values, our result (146°C to 148°C) seems reasonable when considering that the syndiotacticity level lies in the range of 75% to 77%.

As can be seen, the observed T_m° values exhibit a strong correlation with the syndiotacticity in the samples. In an attempt to correlate the dependence of observed T_m° values as a function of syndiotacticity level, Miller[22] modified the original Flory theory for the depression of melting point in copolymers[23,24] to be used in this fashion, and it has been applied by several authors.[12,17,19] The model assumes that a s-PP chain has a random arrangement of syndiotactic dyads, which are crystallizable, and isotactic ones, which are not. Mathematically, this model reads

$$\frac{1}{T_m^\circ} - \frac{1}{(T_m^\circ)_{100\%}} = -\left(\frac{R}{\Delta H_f^\circ}\right) \ln p_r, \qquad (14)$$

where $(T_m^\circ)_{100\%}$ and ΔH_f° are the equilibrium melting temperature and the equilibrium enthalpy of fusion of a s-PP with 100% syndiotacticity level, respectively. R is the gas constant, and p_r is the fraction of the monomer units that are syndiotactically bonded. In this case, p_r is substituted by the racemic dyads [*%r*].

According to eq. (14), $(T_m^\circ)_{100\%}$ can readily be calculated if all other variables are known. The only parameter that we have a problem with is ΔH_f°, due to the scattering in the reported values, which range from 3.1 kJ mol^{-1} (Ref.12) to 8.3 kJ mol^{-1} (Ref.13). Most recent studies have reported ΔH_f° values in the range of 7.7 kJ mol^{-1} (Ref. 18) to 8.0 kJ mol^{-1} (Ref. 16), which is very close to the value of 8.3 kJ mol^{-1} reported earlier by Haftka and Konnecke.[13] In this study, we prefer to use the ΔH_f° value of 8.0 kJ mol^{-1} (190.4 J g^{-1}) in our calculation, the result of which is also listed as the last two columns in Table IV. According to Table IV, it is evident that $(T_m^\circ)_{100\%}$ ranges from 163.2°C to 172.9°C (436.3 K to 446.0 K), with the average value of 168.7 ± 4.1°C (441.8 ± 4.1 K). Reported values of $(T_m^\circ)_{100\%}$ in the literature are 220°C[12] and 214°C,[19] which may be overestimated. Comparison of the $(T_m^\circ)_{100\%}$ values may lead to a misleading conclusion, since different authors often use different values of necessary parameters, especially those of p_r and ΔH_f°. Consequently, we have recalculated $(T_m^\circ)_{100\%}$ values using ΔH_f° = 8.0 kJ mol^{-1}, based on data of known [*%r*] available in the literature.[16,17,19] The average calculated values of $(T_m^\circ)_{100\%}$ are 173.5 ± 1.3°C,[16] 165.0 ± 5.1°C,[17] and 173.6 ± 10.9°C.[19] Based on these values, our result seems very reasonable.

We also recalculated the $(T_m^\circ)_{100\%}$ values by using the ΔH_f° value of 8.3 kJ mol^{-1} (196.6 J g^{-1}). The new $(T_m^\circ)_{100\%}$ values were found to lie in the range of 162.6°C to 172.0°C, with the average value of 168.0 ± 4.0°C (441.1 ± 4.0 K). We have also recalculated the $(T_m^\circ)_{100\%}$ values, based on the same data sets considered in the previous paragraph. The average recalculated values of $(T_m^\circ)_{100\%}$ are 173.1 ± 1.0°C,[16] 164.8 ± 5.2°C,[17] and 173.4 ± 10.9°C.[19] On the basis of these calculated values, we are able to conclude that the lower the value of ΔH_f° used in the calculation, the higher the estimated $(T_m^\circ)_{100\%}$ value.

Overall Crystallization Kinetics

Avrami Analysis.

As described previously, DSC is often used to follow the overall isothermal crystallization by measuring the heat flow released during the crystallization process, according to eq. (1). Combined with eq. (2), the relative crystallinity $\theta(t)$ as a function of reaction time t can be determined. Figure 4 illustrates relative crystallinity as a function of time for s-PP#3 samples isothermally crystallized at T_c ranging from 80°C to 95°C. Based on the Avrami model[7] expressed as eq. (3), the data similar to those shown in Figure 4 can be analyzed according to the Avrami equation in its

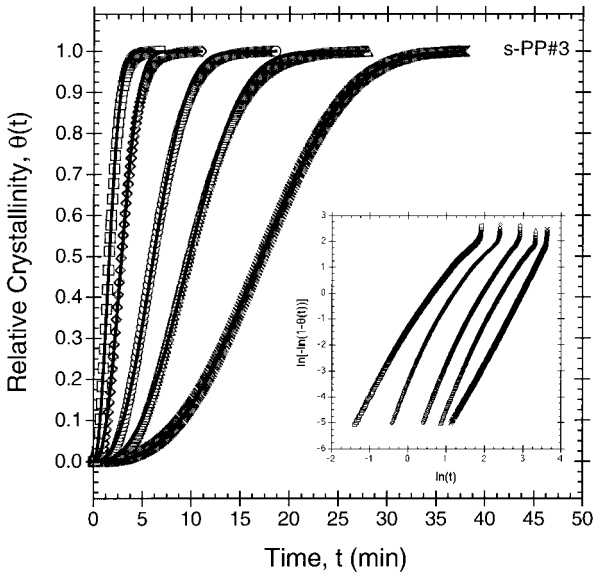

Figure 4 Relative crystallinity as a function of time. Inset: Typical Avrami plots for sample s-PP#3, isothermally crystallized at the specified temperatures: (□) s-PP#4; (◇) s-PP#2; (○) s-PP#3; (△) s-PP#4; (×) s-PP#5.

logarithmic form (i.e., eq. (4)). By performing a least square fit in the range of 10% to 80% relative crystallinity to the Avrami plots such as those shown as the inset figure in Figure 4, the Avrami exponent n and the rate constant k can readily be extracted. In practice, these kinetics parameters, together with eq. (3), can be used to simulate the crystallization process at a given T_c, as shown by the solid lines in Figure 4. The other important parameter is the half-time of crystallization $t_{0.5}$ which is the time taken from the onset of the crystallization until 50% completion, and can be extracted directly from the plot of $\theta(t)$ versus time t. Table IV lists all of the kinetics results for all of the s-PP samples.

Figure 5 shows the plots of the crystallization half-times and their reciprocal values against the crystallization temperature. It is evident that the rate of the crystallization falls in the following sequence: s-PP#5 > s-PP#3 > s-PP#2 > s-PP#4 > s-PP#1, although s-PP#2 seems to crystallize a little bit faster than s-PP#3 at $T_c < 78$°C. It is not possible, at least at this point, to find a reason why these s-PP samples crystallize in that sequence. As is well known, there are a number of factors affecting the crystallization of polymers, including stereoregularity, regioregularity, molecular weight, molecular weight distribution, kind and quantity of nucleation agent used, and presence of impurities. The crystallization behavior, in terms of growth rate and nucleation rate measurement, of these s-PP samples will be investigated more extensively and will be of future publication. With those results, we will be able to conclude with a higher level of confidence what is controlling the isothermal crystallization behavior of these s-PP samples.

According to Table V, the Avrami exponent n does not seem to exhibit a definite overall correlation with T_c, though samples s-PP#3, s-PP#4 and s-PP#5 exhibit a slight gradual increase of n with an increase in crystallization temperature. For all of the s-PP samples, n ranges from 2.01 to 3.27. More specifically, n ranges from 2.41 to 3.22 for s-PP#1; from 2.22 to 2.54 for s-PP#2; from 2.15 to 2.87 for s-PP#3; from 2.05 to 2.88 for s-PP#4; and finally from 2.01 to 3.27 for s-PP#5. Our result seems to fall in a comparable range of the values reported in the literature: 1.91 to 3.34 by Rodriguez-Arnold et al.[16] and 1.81 to 3.86 by Balbontin et al.[19] Along with the plots of $t_{0.5}$ and $t_{0.5}^{-1}$ versus T_c as shown in Figure 5, the plot of the crystallization rate constant k shown in Figure 6, shows that s-PP samples crystallize slower with an increase in T_c, at least in the range of T_c investigated. In our earlier paper,[25] we found that the plot of $t_{0.5}^{-1}$ (for s-PP#1 sample) against T_c exhibits a double bell-shaped curve, while that of the linear growth rate against T_c shows the typical bell-shaped curve. Based on the growth rate theory,[8,9] the bell-shaped curve can be described as a result of the nucleation control effect at high T_c (low undercooling, $\Delta T = (T_m^\circ)_{100\%} - T_c$), and diffusion control at low T_c (high ΔT). It is apparent according to our result shown in Figures 5 and 6 that, within the T_c range of interest, all of the s-PP samples crystallize in the nucleation-controlled range.

Regime Analysis.

As discussed previously in the theoretical section, the growth rate theory[8,9] can also be tested by using t_θ values taken directly from the experimental data, obtained from the DSC experiments. At this moment, we focus only on the relationship between the half-time of crystallization $t_{0.5}$ and crystallization temperature T_c. Since a preliminary observation under a polarized light microscope suggested that all of the s-PP samples crystallize mainly in a three-dimensional, instantaneous fashion, within the T_c range of interest, construction of $\log(t_{0.5}^{-1}) + U^*/2.303R(T_c - T_\infty)$ versus $1/2.303T_c(\Delta T)f$, as shown in Figure 7 for all

Table V Overall Crystallization Kinetics Data for Syndiotactic Polypropylene Samples

	s-PP#1			s-PP#2			s-PP#3			s-PP#4			s-PP#5		
Sample T_c (°C)	$t_{0.5}$ (min)	n	k (min^{-n})	$t_{0.5}$ (min)	n	k (min^{-n})	$t_{0.5}$ (min)	n	k (min^{-n})	$t_{0.5}$ (min)	n	k (min^{-n})	$t_{0.5}$ (min)	n	k ($\text{min}^{-n)}$
60.0	1.67	2.68	1.77×10^{-1}	—	—	—	—	—	—	—	—	—	—	—	—
62.5	1.70	2.74	1.64×10^{-1}	—	—	—	—	—	—	—	—	—	—	—	—
65.0	1.75	2.57	1.66×10^{-1}	—	—	—	—	—	—	—	—	—	—	—	—
67.5	1.83	2.59	1.46×10^{-1}	—	—	—	—	—	—	—	—	—	—	—	—
70.0	1.98	2.68	1.11×10^{-1}	—	—	—	—	—	—	1.24	2.14	4.40×10^{-1}	0.45	2.01	3.58
72.5	2.18	2.73	8.22×10^{-2}	0.81	2.54	1.17	0.84	2.26	1.02	1.33	2.05	3.87×10^{-1}	0.54	2.05	2.40
75.0	2.45	2.80	5.56×10^{-2}	0.94	2.44	7.87×10^{-1}	1.04	2.15	6.30×10^{-1}	1.56	2.10	2.68×10^{-1}	0.63	2.14	1.82
76.5	—	—	—	—	—	—	—	—	—	—	—	—	0.69	2.21	1.57
77.5	2.92	2.97	2.88×10^{-2}	1.19	2.38	4.53×10^{-1}	1.18	2.11	4.89×10^{-1}	1.92	2.11	1.72×10^{-1}	0.72	2.29	1.47
80.0	3.50	3.07	1.47×10^{-2}	1.67	2.33	2.07×10^{-1}	1.58	2.17	2.53×10^{-1}	2.69	2.13	8.25×10^{-2}	0.88	2.37	9.09×10^{-1}
82.5	4.81	3.22	4.36×10^{-3}	2.47	2.22	9.13×10^{-2}	1.96	2.34	1.40×10^{-1}	3.15	2.14	5.83×10^{-2}	1.16	2.57	4.62×10^{-1}
85.0	5.78	3.05	3.30×10^{-3}	3.47	2.35	3.66×10^{-2}	2.82	2.48	5.14×10^{-2}	4.26	2.21	2.78×10^{-2}	1.48	2.69	2.32×10^{-1}
86.0	—	—	—	—	—	—	—	—	—	5.40	2.23	1.60×10^{-2}	1.85	2.88	1.14×10^{-1}
87.5	7.65	2.97	1.66×10^{-3}	4.58	2.36	1.88×10^{-2}	3.85	2.49	2.35×10^{-2}	7.32	2.23	8.04×10^{-3}	2.11	2.76	8.47×10^{-2}
88.0	—	—	—	—	—	—	—	—	—	7.44	2.13	9.48×10^{-3}	—	—	—
90.0	11.40	2.96	5.19×10^{-4}	7.32	2.40	5.72×10^{-3}	6.08	2.67	5.48×10^{-3}	9.80	2.52	2.21×10^{-3}	3.61	2.75	1.99×10^{-2}
91.5	—	—	—	—	—	—	—	—	—	—	—	—	4.59	2.88	8.45×10^{-3}
92.5	19.40	2.47	4.39×10^{-4}	13.48	2.25	1.95×10^{-3}	9.71	2.74	1.33×10^{-3}	16.35	2.57	5.35×10^{-4}	6.16	2.98	3.02×10^{-3}
95.0	28.30	2.41	2.23×10^{-4}	21.57	2.32	5.68×10^{-4}	17.23	2.87	1.98×10^{-4}	30.37	2.88	3.76×10^{-5}	10.89	3.09	4.37×10^{-4}
97.5	—	—	—	—	—	—	—	—	—	—	—	—	15.34	3.27	9.32×10^{-5}

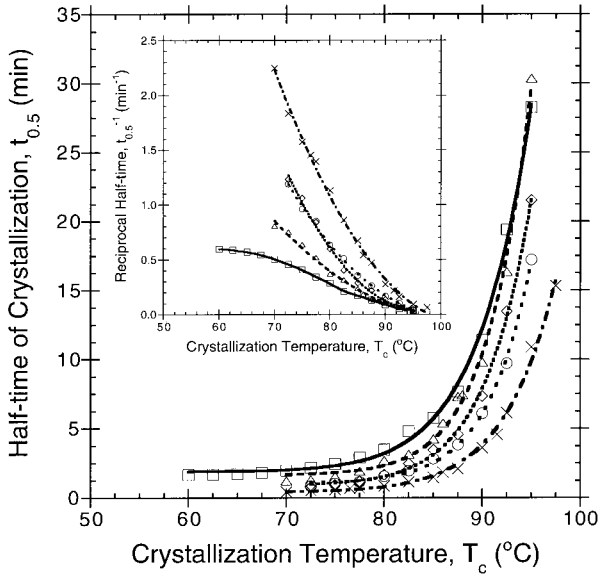

Figure 5 Relative crystallinity as a function of crystallization temperatures. Inset: Reciprocal half-time as a function of crystallization temperature. (□) s-PP#4; (◇) s-PP#2; (○) s-PP#3; (△) s-PP#4; (×) s-PP#5.

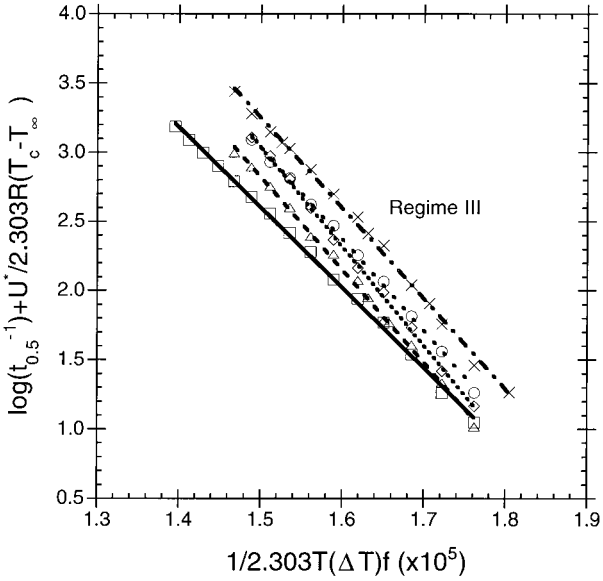

Figure 7 Analysis of the half-times of crystallization based on the modified growth rate theory for the s-PP samples: (□) s-PP#4; (◇) s-PP#2; (○) s-PP#3; (△) s-PP#4; (×) s-PP#5.

of the s-PP samples, serves as the regime test. The parameters used are as follows: $T_\infty = 237$ K ($T_g = 267$ K), $(T_m^\circ)_{100\%} = 441.8$ K, and $U^* = 6{,}276$ J mol^{-1}. It is apparent that the bulk of the data for all of the s-PP samples fit a straight line, with the correlation coefficients r^2 of 0.998 or better. Since earlier reports[16,25–27] have suggested that the regime II → regime III transition should occur at $T_c \approx 110$°C (i.e., $\Delta T \approx 50$°C), we can conclude with a high level of confidence that our data, in the T_c range of interest, represent crystallization in regime III. From the slopes of the plots, the nucleation exponents K_g are found to range from 5.69×10^5 K^2 to 7.03×10^5 K^2.

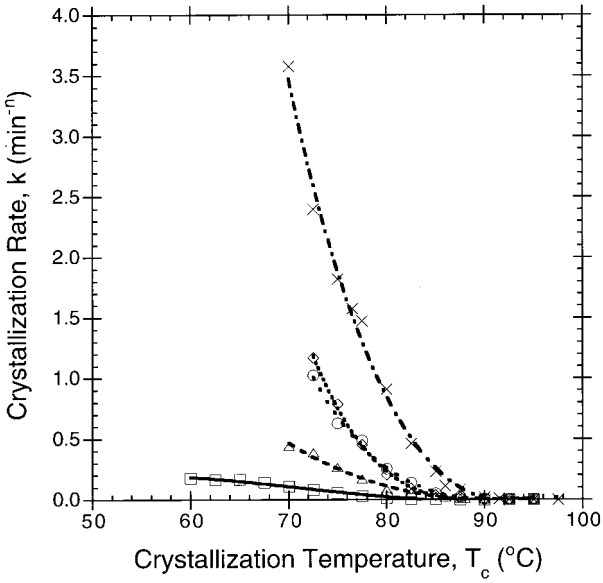

Figure 6 Avrami crystallization rate constant as a function of crystallization temperatures for the s-PP sample: (□) s-PP#4; (◇) s-PP#2; (○) s-PP#3; (△) s-PP#4; (×) s-PP#5.

Once K_g values have been determined, other parameters characteristic of crystal growth can be estimated. First, $\sigma\sigma_e$ can be calculated from eq. (8), provided that other parameters are known. By referring to eq. (8), the only unknown parameter is the layer thickness b_0 which can be estimated from the unit cell parameters. It is therefore imperative to know the crystallographic form and lattice dimensions of the s-PP samples, crystallized in the temperature range of interest. Based on our WAXD results,[28] it is obvious that all of the s-PP samples crystallize in the high temperature orthorhombic form II (Cell II) as determined by Lotz and coworkers,[29] especially when $T_c < 110$°C. The unit cell of this orthorhombic modification occupies the space group $Pca2_1$, with the axis dimensions: $a = 14.50$ Å, $b = 5.60$ Å, and $c = 7.40$ Å. This structure is particularly characterized by the existence of helices of opposite hands with chain axes in $(0, 0, z)$ and $(\frac{1}{2}, 0, z)$.

Table VI Input Parameters for Calculation of Parameters Characteristic of Crystal Growth

Parameter	Value	Remarks
Heat of fusion, ΔH_f°	1.77×10^9 erg cm^{-3}	Ref. 16 and Ref. 29
Glass transition temperature, T_g	−6.1°C or 267.0 K	This work
Equilibrium melting temperature, $(T_m^\circ)_{100\%}$	168.7°C or 441.8 K	This work
Boltzmann's constant, k	1.380×10^{-16} erg molecule^{-1} K^{-1}	
For (010) growth plane		
Molecular width, a_0	7.25×10^{-8} cm	Estimated from Ref. 29
Layer thickness, b_0	5.60×10^{-8} cm	Estimated from Ref. 29
Cross-sectional area of chain, a_0b_0	4.06×10^{-15} cm^2	Estimated from Ref. 29
Lateral surface free energy, σ	11.3 erg cm^{-2}	From $\sigma = 0.1\Delta H_f^\circ(a_0b_0)^{0.5}$
For (200) growth plane		
Molecular width, a_0	5.60×10^{-8} cm	Estimated from Ref. 29
Layer thickness, b_0	7.25×10^{-8} cm	Estimated from Ref. 29
Cross-sectional area of chain, a_0b_0	4.06×10^{-15} cm^2	Estimated from Ref. 29
Lateral surface free energy, σ	11.3 erg cm^{-2}	From $\sigma = 0.1\Delta H_f^\circ(a_0b_0)^{0.5}$

By assuming that (010) or (200) is the growth plane, we are thus able to estimate the molecular width a_0 and the layer thickness b_0. At this point, we are able to calculate the lateral and fold surface free energy, σ and σ_e, separately, but we have first to estimate the σ value based on the modified Thomas–Staveley equation[30]:

$$\sigma = \alpha\Delta H_f^\circ\sqrt{a_0b_0}, \tag{15}$$

where a_0b_0 is a cross-sectional area of one chain molecule, and α is a universal parameter related to the chemical nature of the polymer, and often taken to be 0.1. Now, the fold surface free energy σ_e can be calculated from $\sigma\sigma_e/\sigma$ (cf. $\sigma\sigma_e$ is evaluated from K_g according to eq. (8)). Once the σ_e parameter has been calculated, the average work of chain folding $\bar{q}$, which is defined as

$$\bar{q} = 2a_0b_0\sigma_e, \tag{16}$$

can also be calculated. All of the input parameters necessary for the calculation based on the growth rate theory and the results of the calculation for all of the s-PP samples are listed separately in Tables VI and VII.

According to Table VI, the lateral surface free energy σ is estimated to be 11.3 erg cm^{-2} (mJ m^{-2}) for both (010) and (200) growth planes. This value is in a good agreement with the reported value of 11 erg cm^{-2} by Rodriguez–Arnold et al.,[27] and this value is also close to those estimated for isotactic polypropylene (i-PP) and polyethylene (HDPE),[26] which are 11.5 erg cm^{-2} and 11.1 to 14.1 erg cm^{-2}, respectively. According to the last four columns in Table VII where the half-time of crystallization $t_{0.5}$ was used in the analysis of the regime crystallization, the fold surface free energy σ_e lies in the range of 124.5 to 153.9 erg cm^{-2}, when assuming that (010) is the growth plane, and 96.2 to 118.9 erg cm^{-2}, when assuming that (200) is the growth plane. The work of chain folding was also calculated and was found to be in the range of 14.6 to 18.0 kcal mol^{-1} when assuming that (010) is the growth plane, and 11.2 to 13.9 kcal mol^{-1} when assuming that (200) is the growth plane.

Since these values seem rather high when comparing to the values estimated (σ_e = 49.9 erg cm^{-2} and $\bar{q}$ = 5.8 kcal mol^{-1}) by Clark and Hoffman,[26] and the reported values (σ_e = 42–47 erg cm^{-2} and $\bar{q}$ = 4.8–5.7 kcal mol^{-1}) by Rodriguez–Arnold et al.,[27] we now have to question whether or not our calculation was correct. We therefore tried to confirm our calculation by reevaluating our previous growth rate data (for s-PP#1)[25] and those by Miller and Seeley,[12] using the same input parameters as used in this paper, and found that, evaluated from growth data, σ_e lies in the range of 75.8 to 85.8 erg cm^{-2}, when assuming that (010) is the growth plane, and 54.6 to 61.7 erg cm^{-2}, when assuming that (200) is the growth plane. Likewise, was found to be in the range of 8.9 to 10.0 kcal mol^{-1} when assuming that (110) is the growth plane, and 6.4 to 7.2 kcal mol^{-1} when assuming that (200) is the growth plane. According to these values, we think that there is nothing wrong with our calculation procedure in

Table VII Analysis of the Crystallization Times t_θ Based on the Modified Growth Rate Theory

t_θ (Sample)	$t_{0.1}$				$t_{0.2}$				$t_{0.5}$			
	K_g (K^2)	$\sigma\sigma_e$ ($erg^2\ cm^{-4}$)	σ_e ($erg\ cm^{-2}$)	$\bar{q}$ ($kcal\ mol^{-1}$)	K_g (K^2)	$\sigma\sigma_e$ ($erg^2\ cm^{-4}$)	σ_e ($erg\ cm^{-2}$)	$\bar{q}$ ($kcal\ mol^{-1}$)	K_g (K^2)	$\sigma\sigma_e$ ($erg^2\ cm^{-4}$)	σ_e ($erg\ cm^{-2}$)	$\bar{q}$ ($kcal\ mol^{-1}$)
For (010) growth												
s-PP#1	5.80×10^5	1433.6	127.0	14.8	5.82×10^5	1438.2	127.5	14.9	5.69×10^5	1405.3	124.5	14.6
s-PP#2	7.11×10^5	1755.0	155.5	18.2	7.13×10^5	1759.7	155.9	18.2	7.03×10^5	1737.1	153.9	18.0
s-PP#3	7.00×10^5	1728.4	153.2	17.9	6.86×10^5	1694.1	150.1	17.5	6.49×10^5	1603.5	142.1	16.6
s-PP#4	6.99×10^5	1726.1	153.0	17.9	6.89×10^5	1701.7	150.8	17.6	6.57×10^5	1623.0	143.8	16.8
s-PP#5	7.01×10^5	1731.1	153.4	17.9	6.81×10^5	1682.1	149.1	17.4	6.40×10^5	1580.8	140.1	16.4
For (200) growth plane												
s-PP#1	5.80×10^5	1107.3	98.1	11.5	5.82×10^5	1110.9	98.4	11.5	5.69×10^5	1085.5	96.2	11.2
s-PP#2	7.11×10^5	1355.6	120.1	14.0	7.13×10^5	1359.2	120.4	14.1	7.03×10^5	1341.8	118.9	13.9
s-PP#3	7.00×10^5	1335.0	118.3	13.8	6.86×10^5	1308.5	116.0	13.6	6.49×10^5	1238.6	109.8	12.8
s-PP#4	6.99×10^5	1333.2	118.1	13.8	6.89×10^5	1314.4	116.5	13.6	6.57×10^5	1253.6	111.1	13.0
s-PP#5	7.01×10^5	1337.1	118.5	13.9	6.81×10^5	1299.3	115.1	13.5	6.40×10^5	1221.0	108.2	12.6

the present paper. The discrepancy between the growth parameters analyzed from the bulk kinetics and those from the growth kinetics may result from the fact that the bulk kinetics also includes the nucleation kinetics, which is totally ignored when growth kinetics was analyzed.

In Table VII, we have also listed growth parameters analyzed from crystallization times at 10% and 20% relative crystallinity, $t_{0.1}$ and $t_{0.2}$, respectively. The results seem to decrease in value corresponding to the crystallization times, t_θ, in the following order: $t_{0.1} > t_{0.2} > t_{0.5}$.

Construction of Crystallization Rate Function

Measurement of the crystallization times t_θ is not always possible especially in the lower crystallization temperature range. According to the growth theory, crystallization of polymers at low temperatures or high degrees of undercooling usually occurs in regime III. If the crystallization time data in this temperature range are available, they can be used to estimate the crystallization time values at other temperatures. This can done by the use of eq. (10), which states the relationship of the reciprocal value of the crystallization time and the temperature. Provided that T_m° and T_g are known, the only unknown parameters are A_1G_0 and K_g, which can readily be obtained from the regime plot where A_1G_0 is the antilogarithmic value of the y-intercept ($A_1G_0 = 10^{(y-\text{intercept value})}$) and K_g is the negative value of the slope ($K_g = -\text{slope}$). This can be demonstrated by taking the case of s-PP#1 as an example.

According to the regime plot (analyzed for the half-time data) of the s-PP#1 sample, the values of A_1G_0 and K_g are 2.06×10^{11} and 5.69×10^5, respectively. Substitution of these values into eq. (10) leads to the expression of the half-time of crystallization as a function of temperature:

$$(t_{0.5}^{-1})_{\text{III}}\ (\text{min}^{-1}) = 2.06 \times 10^{11} \times \exp\left(-\frac{754.83}{(T_c - T_\infty)} - \frac{5.69 \times 10^5}{T_c(\Delta T)f} \right). \quad (17)$$

The expressions of crystallization times as a function of temperature for all of the samples can also be obtained in the similar fashion as shown above. Figure 8 shows both the experimental and predicted values of the reciprocal half-times as a function of temperature for all of the s-PP samples. Apparently, the maxima in all of the plots occur near 60°C.

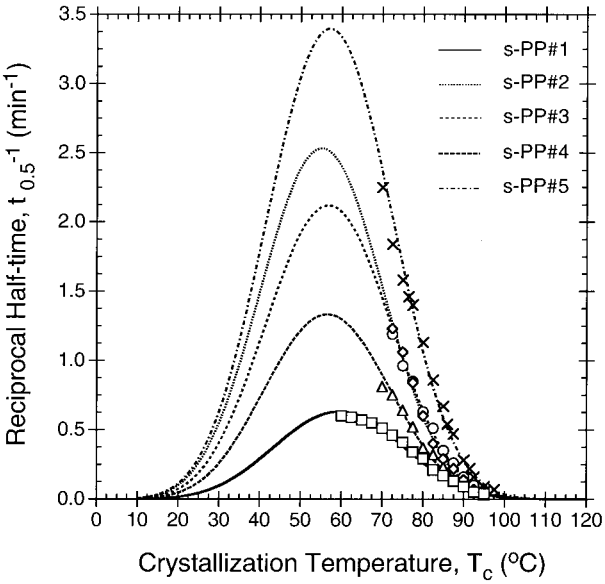

Figure 8 Reciprocal half-time as a function of crystallization temperature for the s-PP samples showing the comparison to the calculated curves based on eq. (10) (lines): (□) s-PP#4; (◇) s-PP#2; (○) s-PP#3; (△) s-PP#4; (×) s-PP#5.

Kinetic Crystallizability.

The temperature dependence of the crystallization half-times was introduced as early as in 1967 by Ziabicki[31–33] and can be described by a Gaussian function of the form:

$$t_{0.5}^{-1} = (t_{0.5})_{\min}^{-1} \exp\left[-4 \ln 2 \, \frac{(T_c - T_{\max})^2}{D^2} \right], \quad (18)$$

where $T_{\max}$ is the temperature where the crystallization is the maximum, $(t_{0.5})_{\min}$ the crystallization half-time at $T_{\max}$, and D the half-width of the crystallization rate (the reciprocal value of the crystallization half-time) curve. With use of the isokinetic approximation, integration of eq. (18) over the whole range of temperatures in which crystallization may occur ($T_g < T < T_m^\circ$) leads to an important characteristic value describing the crystallization ability of the polymer, namely the kinetic crystallizability G:

$$\int_{T_g}^{T_m^\circ} t_{0.5}^{-1}(T) \, dT \approx \frac{1.064D}{(t_{0.5})_{\min}} = G. \quad (19)$$

In practice, $T_{\max}$, $(t_{0.5})_{\min}$, and D may be measured from a curve such as that shown in Figure 8. Table VIII lists the $T_{\max}$, $(t_{0.5})_{\min}$, D, and G values for all of the s-PP samples. The characteristic values of some other polymers[33] are also listed for comparison. The practical meaning of the G parameter is to characterize the ability of the polymer in crystallizing when it is cooled from the melting temperature to the glass transition temperature at a constant cooling rate.[33] The higher the G values, the more readily the polymer crystallizes. Based on the G values listed in Table VIII, the crystallization ability of the s-PP samples falls in the following order: s-PP#5 > s-PP#2 > s-PP#3 > s-PP#4 > s-PP#1. When comparing with some other polymers listed in Table VIII, the crystallization ability of these polymers fall in the following sequence: Nylon 66 > i-PP > Nylon 6 > s-PP > i-PS.

CONCLUSIONS

The average glass transition temperature for all of the s-PP samples used was determined to be

Table VIII Kinetic Characteristics of Syndiotactic Polypropylene Samples and Some Other Polymers

	T_m° (°C)	T_g (°C)	$T_{\max}$ (°C)	$(t_{0.5})_{\min}$ (sec)	D (°C)	G (°C sec^{-1})
s-PP#1	146.1	−6.1	60.0	95.2	36.9	0.41
s-PP#2	146.6	−6.0	55.0	23.7	34.7	1.56
s-PP#3	148.3	−6.5	57.0	28.3	35.6	1.34
s-PP#4	146.4	−5.6	56.5	45.0	35.5	0.84
s-PP#5	146.4	−6.5	57.0	17.7	35.6	2.14
i-PS[a]	240	100	170	185	40	0.16
Nylon 6[a]	228	45	146	5	46	6.8
Nylon 66[a]	264	45	150	0.42	80	139
i-PP[a]	180	−20	65	1.25	60	35

[a] Data taken from Table 2.5 in Ref. 33.

-6.1 ± 0.4°C (267.0 ± 0.4 K). Observation of subsequent melting of the s-PP samples after isothermal crystallization at specified crystallization temperatures showed the existence of two endotherms whose position on the temperature axis and heat absorbed depended significantly on the crystallization temperature and the heating rate used. The result suggested that, at least in the crystallization range of interest (from 60°C to 97.5°C), the low-melting endotherms correspond to the melting of crystalline aggregates formed at specified crystallization temperature, whereas the high-melting ones are the result of the melting of crystalline aggregates that formed by recrystallization during heating. The typical Hoffman–Weeks extrapolation suggested that the equilibrium melting temperature T_m° lies in the range of 146.1°C to 148.3°C (419.3 K to 421.4 K). Finally, the equilibrium melting temperature of 100% syndiotacticity $(T_m^\circ)_{100\%}$ was estimated to be 168.7 ± 4.1°C (441.8 ± 4.1 K), which is the average value determined from the s-PP samples studied.

The half-times of crystallization $t_{0.5}$ revealed that the rate of the crystallization for all of the s-PP samples is in the following order: s-PP#5 > s-PP#3 > s-PP#2 > s-PP#4 > s-PP#1. The Avrami index n does not seem to have a significant relationship with the crystallization temperature, at least in the temperature range of interest, and ranges from 2.01 to 3.27. The crystallization rate constant k agrees extremely well with what was observed by the half-time of crystallization. The plot of $\log(t_\theta^{-1}) + U^*/2.303R(T_c - T_\infty)$ against $1/2.303T_c(\Delta T)f$, serving as a regime test based on the growth rate theory, for t_θ at (= 0.10, 0.20, and 0.50 clearly showed straight lines for all of the s-PP samples. It was assumed that s-PP samples crystallize in regime III within the studied temperature range (60°C to 97.5°C).

The ability of the s-PP samples to crystallize was determined by the kinetic crystallizability parameters G, which ranges from 0.41°C s^{-1} to 2.14°C s^{-1}. Based on this parameter, the crystallizability of all of the s-PP samples is in the following sequence: s-PP#5 > s-PP#2 > s-PP#3 > s-PP#4 > s-PP#1. Comparison with some other polymers reveals that syndiotactic polypropylene crystallizes much slower than Nylon 6, isotactic polypropylene, and Nylon 66, while it crystallizes faster than isotactic polystyrene.

We thank Dr. Joseph Schardl of Fina Oil and Chemical Company in Dallas, Texas, for supplying the s-PP samples, and Dr. Roger A. Phillips and his co-workers of Montell SA, Inc. in Elkton, Maryland, for performing sample characterizations.

REFERENCES

1. Ziegler, K.; Holzkamp, E.; Breil, H.; Martin, H. Angew Chem 1955, 67, 541.
2. Natta, G. J Polym Sci 1955, 16, 143.
3. Natta, G.; Pino, P.; Corradini, P.; Danusso, F.; Mantica, E.; Mazzanti, G.; Moraglio, G. J. Am Chem Soc 1955, 77, 1708.
4. Natta, G.; Pasquon, I.; Zambelli, A. J. Am Chem Soc 1962, 84, 1488.
5. Boor, J., Jr.; Youngman, E. A. J Polym Sci Polym Chem 1966, 4, 1861.
6. Ewen, J. A; Johns, R. L.; Razavi, A.; Ferrara, J. D. J Am Chem Soc 1988, 110, 6255.
7. Avrami, M. J Chem Phys 7, 1939, 1103; 1940, 8, 212; 1941, 9, 177.
8. Hoffman, J. D.; Davis, G.T.; Lauritzen, J. I., Jr. in Treatise on Solid State Chemistry, Vol. 3, Plenum Press, New York, 1976, Chapter 7.
9. Hoffman, J. D. Polymer, 1983, 24, 3.
10. Hoffman, J. D.; Weeks, J. J. J Res Natl Bur Stand 1962, A66, 13.
11. Mathot, V. B. F. in Calorimetry and Thermal Analysis of Polymers, Carl Hanser Verlag, Munich, 1994, p 173.
12. Miller, R. L.; Seeley, E. G. J Polym Sci Polym. Phys 1982, 20, 2297.
13. Haftka, S.; Könnecke, K. J Macromol. Sci Phys 1991, B30(4), 319.
14. Eckstein, A.; Friedrich, C.; Lobbrecht, A.; Spitz, R.; Mülhaupt, R. Acta Polymer 1997, 48, 41.
15. Marigo, A.; Marega, C.; Zannetti, R.; Celli, A.; Paganetto, G. Macromol Rapid Commun 1994, 15, 225.
16. Rodriguez-Arnold, J.; Zhang, A.; Cheng, S. Z. D.; Lovinger, A. J.; Hsieh, E. T.; Chu, P.; Johnson, T. W.; Honnell, K. G.; Geerts, R. G.; Palackal, S. J.; Hawley, G. R.; Welch, M. B. Polymer 1994, 35(9), 1884.
17. Uehara, H.; Yamazaki, Y.; Otake, C.; Kanamoto, T. Kobunshi Ronbunshu 1994, 51(9), 597.
18. Schmidtke, J.; Strobl, G.; Thurn-Albrecht, T. Macromolecules 1997, 30, 5804.
19. Balbontin, G.; Dainelli, D.; Galimberti, M.; Paganetto, G. Makromol Chem 1992, 193, 693.
20. Boor, J., Jr.; Youngman, E. A. J Polym Sci Polym. Lett 1965, 3, 577.
21. Youngman, E. A.; Boor, J., Jr. Macromol Rev 1967, 2, 33.
22. Miller, R. L. J Polym Sci 1962, 57, 975.
23. Flory, P. J. J Chem Phys 1949, 17, 223.
24. Flory, P. J. Trans Faraday Soc 1955, 51, 848.
25. Supaphol, P.; Hwu, J.-J.; Phillips, P. J.; Spruiell, J. E. The Proceedings of the 55th Annual Technical

Conference (ANTEC), Society of Plastics Engineers, 1997, 1759.
26. Clark, E. J.; Hoffman, J. D. Macromolecules 1984, 17, 878.
27. Rodriguez-Arnold, J.; Bu, Z.; Cheng, S. Z. D.; Hsieh, E. T.; Johnson, T. W.; Geerts, R. G.; Palackal, S. J.; Hawley, G. R.; Welch, M. B. Polymer 1994, 35(24), 5194.
28. Supaphol, P.; Spruiell, J. E. in preparation.
29. Lotz, B.; Lovinger, A. J.; Cais, R. E. Macromolecules 1988, 21, 2375.
30. Thomas, D. G.; Staveley, L. A. K. J Chem Soc 1952, 4569.
31. Ziabicki, A. Appl Polym Symp 1967, 6, 1.
32. Ziabicki, A Polymery 1967, 12, 405.
33. Ziabicki, A in Fundamentals of Fiber Spinning, John Wiley & Sons, New York, 1976, p 114.